© 2014. Published by The Company of Biologists Ltd | The Journal of Experimental Biology (2014) 217, 1993-2003 doi:10.1242/jeb.098863

RESEARCH ARTICLE

Skeletal muscle fuel selection occurs at the mitochondrial level

Sarah Kuzmiak-Glancy[1] and Wayne T. Willis[1,2,*]

ABSTRACT

Mammals exponentially increase the rate of carbohydrate oxidation as exercise intensity rises, while birds combust lipid almost exclusively while flying at high percentages of aerobic capacity. The fuel oxidized by contracting muscle depends on many factors: whole-body fuel storage mass, mobilization, blood transport, cellular uptake, and substrate selection at the level of the mitochondrion. We examined the fuel preferences of mitochondria isolated from mammalian and avian locomotory muscles using two approaches. First, the influence of substrates on the kinetics of respiration ($K_{m,ADP}$ and V_{max}) was evaluated. For all substrates and combinations, $K_{m,ADP}$ was generally twofold higher in avian mitochondria. Second, fuel competition between pyruvate, glutamate and/or palmitoyl-L-carnitine at three levels of ATP free energy was determined using the principle of mass balance and the measured rates of O_2 consumption and metabolite accumulation/utilization. Avian mitochondria strongly spared pyruvate from oxidation when another substrate was available and fatty acid was the dominant substrate, regardless of energy state. Mammalian mitochondria exhibited some preference for fatty acid over pyruvate at lower flux (higher energy state), but exhibited a much greater tendency to select pyruvate and glutamate when available. Studies in sonicated mitochondria revealed twofold higher electron transport chain electron conductance in avian mitochondria. We conclude that substantial fuel selection occurs at the level of the mitochondrial matrix and that avian flight muscle mitochondria are particularly biased toward the selection of fatty acid, possibly by facilitating high β-oxidation flux by maintaining a more oxidized matrix.

KEY WORDS: Skeletal muscle mitochondria, Fuel selection, Mitochondrial function

INTRODUCTION

Post-absorptive mammals rest at a whole-body respiratory quotient (RQ) near 0.80, with fat providing ~2/3 of the energy substrates (Brooks and Donovan, 1983; Willis et al., 2005). Skeletal muscle arterio-venous RQ is yet lower, showing an even stronger bias toward fat oxidation in resting muscle (Dagenais et al., 1976). Fasted birds generally rest at a lower whole-body RQ. For example, 2.8 g hummingbirds rest at a RQ of 0.72 (Suarez et al., 1990), 23 g sparrows at 0.71 (Walsberg and Wolf, 1995) and 480 g ravens at 0.80 (Hudson and Bernstein, 1983). These observations taken together support the concept that, in the post-absorptive state, resting mammalian and avian skeletal muscle cells preferentially select lipid as their oxidative substrate.

Most mammalian and avian skeletal muscle cells rest at very low fractions of their aerobic capacity, probably less than 1%. Studies in several mammalian species have clearly demonstrated the enormous aerobic scope of mammalian skeletal muscle. For example, human muscle, which has been shown to rest at about 2 ml O_2 min^{-1} kg^{-1} (Dagenais et al., 1976; Zurlo et al., 1990), may achieve maximum O_2 consumption rates in excess of 300 ml min^{-1} kg^{-1} (Andersen and Saltin, 1985; Richardson et al., 1993). The metabolic control signals underlying this expansive dynamic range, while not definitively understood, have been well characterized in many mammalian species using several methodologies (Chance et al., 1985; Connett, 1987; Jeneson et al., 1995). Contractile activity elevates the rate of ATP hydrolysis and results in the cytosolic accumulation of the ATP hydrolysis products ADP and inorganic phosphate (P_i), and thus decreased (less negative) ATP free energy (ΔG_{ATP}). A nearly linear relationship between O_2 consumption rate ($\dot{V}_{O_2}$) and ΔG_{ATP}, consistent with simple feedback control, has been repeatedly demonstrated both *in vivo* (Kushmerick et al., 1992; Jeneson et al., 1995) and in isolated mitochondria *in vitro* (Rottenberg, 1973; Davis and Davis-van Thienen, 1989; Willis and Jackman, 1994; Messer et al., 2004; Glancy et al., 2008; Glancy et al., 2013). Because of the near-equilibrium maintained by the creatine kinase and adenylate kinase reactions, *in vivo* P_i rises nearly linearly with muscle $\dot{V}_{O_2}$, while ADP, and particularly AMP, rise more abruptly as high fractions of the aerobic capacity are approached (Funk et al., 1989; Foley et al., 1991). All three of these energy phosphates exert strong and independent positive modulation on important rate-controlling enzymes of the glycogenolytic pathway (Stanley and Connett, 1991; Lambeth and Kushmerick, 2002). As both ADP and AMP rise exponentially as whole-body maximum O_2 consumption rate ($\dot{V}_{O_2,max}$) is approached, this energy phosphate control of mitochondrial oxidative phosphorylation appears consistent with the observation that mammalian muscle exponentially increases the recruitment of carbohydrate into the fuel supply as exercise intensity rises toward $\dot{V}_{O_2,max}$ (Brooks and Mercier, 1994; Roberts et al., 1996). At and above moderate exercise intensity, mammalian muscle remains critically dependent on carbohydrate even in the absence of high blood lactate or glucose concentrations (O'Brien et al., 1993), and actively suppresses fat oxidation at high ATP turnover rates (Romijn et al., 1995; Sidossis and Wolfe, 1996). Indeed, glycogen depletion precipitates the failure of mammalian muscle contractile output (Wahren et al., 1971; Baldwin et al., 1973; Fitts et al., 1975), despite the presence of a vast lipid energy reserve.

In profound contrast, birds fly at high percentages of $\dot{V}_{O_2,max}$, combusting fat at nearly the complete exclusion of carbohydrate (Rothe et al., 1987; Suarez et al., 1990), which indicates that the fuel selection of highly active avian muscle categorically differs from that of mammals. Moreover, avian skeletal muscle must achieve extremely high aerobic energy turnover to support flight and is equipped with a mitochondrial density 2–5 times that of mammalian skeletal muscle to do so. Pigeon pectoralis muscle provides an informative example: 300 g pigeons fly at a whole-body $\dot{V}_{O_2}$ of roughly 200 ml min^{-1} kg^{-1} body mass (Rothe et al., 1987), and the pectoralis, which is about 10% of body mass (30 g), must account for well over half of this. This conservative estimation gives a muscle tissue $\dot{V}_{O_2}$ of at least 3000 ml min^{-1} kg^{-1} muscle, almost all

[1]School of Life Sciences, Arizona State University, Tempe, AZ 85287, USA. [2]Mayo Clinic, Scottsdale, AZ 85259, USA.

*Author for correspondence (waynewillis@asu.edu)

Received 21 October 2013; Accepted 19 February 2014

The Journal of Experimental Biology (2014) doi:10.1242/jeb.098863

List of symbols and abbreviations

A	arsenite
$[ADP]_f$	'free' (not bound) ADP concentration
CK	creatine kinase
CPT-I	carnitine palmitoyltransferase I
Cr	creatine
ETC	electron transport chain
G	glutamate
G3P	glycerol 3-phosphate
IDH	NAD^+-linked isocitrate dehydrogenase
J_{e-}	electron current
J_O	rate of mitochondrial oxygen consumption
K_{eq}	equilibrium constant
$K_{m,ADP}$	kinetic control of J_O by $[ADP]_f$ alone
M	malate
MDH	malate dehydrogenase
OAA	oxaloacetate
2-OG	2-oxoglutarate
OGDH	2-oxoglutarate dehydrogenase
P	pyruvate
PC	palmitoyl-L-carnitine
PCr	phosphocreatine
PDH	pyruvate dehydrogenase
PDH_A	active (dephosphorylated) pyruvate dehydrogenase
P_i	inorganic phosphate
R	ideal gas constant
RER	respiratory exchange ratio
RM	respiration medium
RQ	respiratory quotient
T	temperature in Kelvin
V_{max}	maximum rate in Michaelis–Menten kinetics
$\dot{V}_{O_2}$	O_2 consumption rate
$\dot{V}_{O_2,max}$	maximum O_2 consumption rate
ΔG_{ATP}	ATP free energy
ΔE_h	redox potential difference
ΔE_h:J_O	ETC thermodynamic force:metabolic flow
ΔG_{redox}	redox free energy difference down the ETC
Δp	protonmotive force across the inner mitochondrial membrane

of which goes toward the combustion of lipid, because whole-body RQ is ~0.72 (Rothe et al., 1987). Thus, while mammalian muscle transitions from a lipid-based fuel metabolism at rest to near-complete reliance on carbohydrate as an aerobic maximum perhaps 100-fold higher is approached, avian muscle $\dot{V}_{O_2}$ rising far higher continues to select lipid as its oxidative fuel.

The mechanisms underlying this dramatically different fuel metabolism remain poorly understood. The state 3 (maximum) rate of mitochondrial oxygen consumption, J_O, of pigeon pectoralis mitochondria oxidizing pyruvate is roughly equal to that of palmitoyl-L-carnitine (Rasmussen et al., 2004), and the pioneering work of Suarez et al. showed similar trends in hummingbird pectoralis (Suarez et al., 1986). Data from pectoralis mitochondria of the house sparrow further confirm this avian pattern, as recently reported by our laboratory (Kuzmiak et al., 2012). As pyruvate (carbohydrate) and β-oxidation (fatty acid) pathways elicit equal rates of oxygen consumption, the selection of fatty acid fuel during avian flight cannot be simply explained by a higher catalytic potential for fat oxidation. Moreover, *in vivo* studies on pigeon and hummingbird clearly show that avian muscle exhibits substantial metabolic flexibility under certain conditions. From the complementary pigeon studies of Rothe et al. (Rothe et al., 1987) and Butler et al. (Butler et al., 1977) emerges the concept that a large glycogenolysis initiated by the onset of flight mobilizes carbohydrate carbon as lactate into the blood, as whole-body respiratory exchange ratio (RER) rises toward 1.00 (Butler et al., 1977; Rothe et al., 1987). Continued steady-rate flight over the next 30 min or so results in a progressively falling RER toward a steady-state value near 0.7 (Rothe et al., 1987). Another example of avian metabolic flexibility is the hovering hummingbird, in which whole-body RER promptly rises from near 0.7 to 1.0 when nectar feeding is allowed (Suarez et al., 1990). Mammalian skeletal muscle also exhibits metabolic flexibility as it adjusts fuel selection toward the oxidation of lactate (Mazzeo et al., 1986; Stanley et al., 1986) and glucose (Horowitz et al., 1999; Koutsari and Sidossis, 2003) when these carbohydrate fuels are made available.

The present study focused on the metabolism of mitochondria isolated from the locomotory muscle of a mammal [mixed hindlimb muscle of rat, *Rattus norvegicus* (Berkenhout 1769)] and a bird [pectoralis of house sparrow, *Passer domesticus* (Linnaeus 1758)]. Three fundamental characteristics were studied. (1) In avian muscle, very little is known about the sensitivity of respiratory control (e.g. the relationship between ATP free energy and $\dot{V}_{O_2}$ or the $K_{m,ADP}$ for respiration) or the extent to which the fuel supply available to mitochondria might influence this control sensitivity. We therefore determined this relationship between energy phosphate levels and mitochondrial O_2 consumption rate (J_O) in mitochondria provided with saturating levels of three oxidative substrates: pyruvate, glutamate and palmitoyl-L-carnitine, as well as combinations of these fuels. (2) With these same fuels, we assessed the extent to which fuels competed for oxidation (fuel competition) or simply added together to a higher flux (fuel additivity) at three experimentally fixed levels of ATP free energy (ΔG_{ATP}), −14.0, −13.5 and −13.0 kcal mol^{-1}. (3) Finally, it has been shown that a reduced (high NADH/NAD^+ ratio) mitochondrial matrix strongly inhibits the β-oxidation of fatty acids (Lumeng et al., 1976). Our previous work has shown NADH cytochrome *c* reductase activity is 80% higher in sparrow versus rat skeletal muscle, indicating a greater maximal rate of electron transport chain (ETC) flux in birds than in mammals (Kuzmiak et al., 2012). Because an ETC capable of achieving a given $\dot{V}_{O_2}$ at a low matrix NADH/NAD^+ should provide a competitive advantage for fatty acid to contribute to the oxidative fuel supply, we predicted higher conductance for electron flow down the ETC in avian than in mammalian mitochondria. We therefore evaluated the kinetics of NADH oxidation by the ETC in sonicated mitochondria.

The results show that, with every fuel and fuel combination tested, avian muscle mitochondria control respiration across a wider range of ATP free energy than mammals or, stated in familiar kinetic terms, the avian $K_{m,ADP}$ for respiration was significantly higher. Further, it is clearly shown in both mammalian and avian mitochondria, but especially in the bird, that muscle mitochondria provided with fatty acid suppress pyruvate oxidation more strongly than can be explained by the relative catalytic potentials of the two competing pathways. The findings also demonstrate that glutamate conversion to aspartate (the mitochondrial steps of the malate–aspartate shuttle) suppresses the oxidation of fatty acid in both types of mitochondria, but does so to a much greater extent in mammalian muscle. Finally, as predicted, the electron conductance of avian ETC exceeded that of the mammal, by over 50%.

RESULTS

Isolated mitochondria were of good functional integrity as indicated by high maximal respiration rates and energy coupling. With pyruvate (P) + malate (M) as substrates, state 3 J_O was 753±81 nmol mg^{-1} min^{-1} in rat and 548±9 nmol mg^{-1} min^{-1} in sparrow mitochondria (supplementary material Table S1). The corresponding ADP/O ratios were 2.83±0.15 and 3.00±0.04, and respiratory control ratios were 5.5±0.8 and 5.4±1.0 (supplementary material Table S1).

The Journal of Experimental Biology (2014) doi:10.1242/jeb.098863

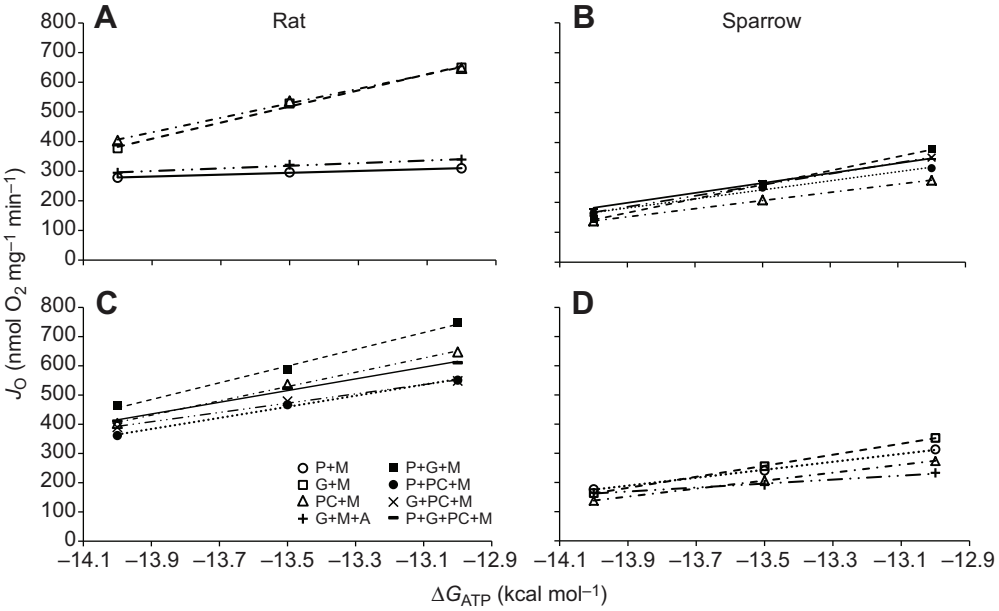

Fig. 1. Oxygen consumption rate (J_O) as a function of ATP free energy (ΔG_{ATP}). (A,B) Data for single fuel combinations for rat (A) and sparrow (B). (C,D) Data for incubations with multiple substrates for rat (C) and sparrow (D). Pyruvate + malate (P+M) is included in both as a reference. Fuel combinations are P+M, G+M, PC+M, G+M+A, P+G+M, P+PC+M, G+PC+M and P+G+PC+M, where: P, pyruvate; M, malate; G, glutamate; PC, palmitoyl-L-carnitine; A, arsenite. *N*=4 rats, *N*=3 sparrows.

Thermodynamic assessment of respiratory control sensitivity

Typically, the relationship between ΔG_{ATP} and J_O is nearly linear. The slope of this relationship is one index of respiratory control sensitivity and can be described as the elasticity of mitochondrial J_O to ΔG_{ATP}. Near-linear relationships were observed in mitochondria oxidizing all fuel combinations in the present study (Fig. 1), and the slopes, or elasticities, often differed depending on species and substrate (Table 1). For example, rat mitochondria exhibited similar slopes with all substrates with the notable exceptions of palmitoyl-L-carnitine (PC) + M and glutamate (G) + M + arsenite (A) (Table 1). Specifically, elasticity with P+M was over 7 and 5 times greater than that with PC+M and G+M+A, respectively (Table 1). Sparrow mitochondria exhibited similar force:flow slopes for all substrates with two exceptions: the addition of glutamate to P+M significantly increased the slope by 72% and the addition of arsenite to G+M significantly reduced the slope by about 64% (Fig. 1, Table 1). Indeed, the addition of the 2-oxoglutarate (2-OG) dehydrogenase (OGDH) inhibitor arsenite to mitochondria oxidizing G+M decreased respiration in both species by ~54% at the calculated V_{max} J_O (Table 2). Sparrow mitochondria, however, were slightly less affected by this OGDH inhibition; at ΔG_{ATP} of −13.0 kcal mol^{-1} the G+M+A/G+M ratio was significantly higher in sparrow than in rat (0.66±0.03 and 0.53±0.03, respectively).

Table 1. Mean slopes ± s.e.m. for ΔG_{ATP}:J_O relationships shown in Fig. 1

Fuels	Rat	Sparrow
P+M	245±31	136±18
G+M	280±69	189±11
PC+M	32±11*	136±5
G+M+A	44±14*	68±5
P+G+M	286±18	234±19*
P+PC+M	167±55	152±22
G+PC+M	159±23	184±21
P+G+PC+M	229±24	165±25

ΔG_{ATP}, ATP free energy; J_O, rate of mitochondrial oxygen consumption; P, pyruvate; M, malate; G, glutamate; PC, palmitoyl-L-carnitine; A, arsenite.
*Significantly different from P+M.

Kinetic assessment of respiratory control sensitivity

Using the data set above, the $K_{m,ADP}$ and V_{max} for respiration for each fuel combination were determined from Eadie–Hofstee analysis; these are reported in Table 2. In rat mitochondria, P+M V_{max} was 2.5 times higher than PC+M V_{max} and 2.3 times higher than G+M+A V_{max} (Table 2). In contrast, in sparrow P+M V_{max} was similar to PC+M V_{max}, and also to all other substrate combinations with one exception. Specifically, the addition of glutamate to P+M almost doubled V_{max} and similarly doubled the $K_{m,ADP}$ (Table 2). In contrast, this addition of glutamate to P+M did not significantly increase V_{max} over P+M alone in rat mitochondria, with the average increase a modest 13% compared to the 96% increase in sparrow mitochondria (Table 2). Importantly, the V_{max} values reported in Table 2, determined using Eadie–Hofstee analysis of steady state conditions established with the creatine kinase energy clamp, are in excellent agreement with state 3 rates determined conventionally with saturating addition of ADP as seen in supplementary material Fig. S1, and also as recently reported by our laboratory (Kuzmiak et al., 2012).

In sparrow mitochondria, no fuel combination $K_{m,ADP}$ was significantly different from the P+M value, with the exception of the much higher $K_{m,ADP}$ observed with P+G+M noted above (Table 2). For all fuel combinations except P+PC+M, sparrow $K_{m,ADP}$ values were significantly higher than rat (Table 2). In rat mitochondria, very low $K_{m,ADP}$ values were observed for fat oxidation (PC+M) and for G+M+A, the mitochondrial steps of the malate–aspartate shuttle (Table 2).

Fuel J_O values across all energy states are reported as a percentage of V_{max} in Table 3. These values represent the mean for all fuel combinations at a given ΔG_{ATP}. At the three clamped energy states (ΔG_{ATP}=−14.0, −13.5 and −13.0 kcal mol^{-1}), average rat J_O were 60, 75 and 86% V_{max}, respectively, while corresponding sparrow values were 36, 53 and 69% V_{max}. J_O/V_{max} values for each fuel combination can be found in supplementary material Table S2.

Fuel utilization

Pyruvate sparing

In sparrow mitochondria under any energetic condition, pyruvate metabolism was strongly suppressed by the addition of any other fuel (Fig. 2). The addition of glutamate, fatty acid or their

Table 2. V_{max} and $K_{m,ADP}$ values determined from Eadie–Hofstee plots of J_O/[ADP] versus J_O

	V_{max} (nmol O_2 mg^{-1} min^{-1})		$K_{m,ADP}$ (μmol l^{-1})	
	Rat	Sparrow	Rat	Sparrow
P+M	810±87	408±50*	16.6±1.3	32.3±1.5*
G+M	825±104	527±38	17.7±3.4	34.3±1.7*
PC+M	321±51‡	414±4	2.3±0.8‡	23.3±3.3*
G+M+A	357±35‡	260±26	4.8±0.4‡	9.9±0.9*
P+G+M	916±54	801±70‡	17.6±3.3	75.3±12.6*,‡
P+PC+M	640±131	465±66	11.9±3.4	30.5±6.8
G+PC+M	626±44	506±79	10.3±1.9	29.7±6.8*
P+G+PC+M	731±107	503±75	12.5±2.7	29.4±4.3*

Values represent means ± s.e.m.
*Significantly different from rat. N=4 rats, N=3 sparrows. ‡Significantly different from P+M in the same species.

combination markedly decreased pyruvate utilization (Fig. 2B) and this suppression was even more pronounced when expressed relative to the oxygen consumption rate (Fig. 2D). In marked contrast, in the rat, suppression of pyruvate utilization was only observed at the highest energy state (ΔG_{ATP}=–14.0 kcal mol^{-1}), which is the energetic condition most similar to the low flux of rest, or when both G and PC were added (Fig. 2C).

The percentage decrease in pyruvate utilization resulting from the addition of palmitoyl-L-carnitine and/or glutamate is shown in Fig. 3A,B. The figure clearly shows that sparrow mitochondria reduce the pyruvate utilized, by roughly 70–80%, when either β-oxidation or the malate–aspartate shuttle, or a combination of the two, is fueled, regardless of energy state. Rat mitochondria also spare pyruvate from oxidation when other fuels are available, but, unlike the sparrow, the extent of pyruvate sparing is highly dependent upon both the energy state (Fig. 3B) and what alternative fuels are available (Fig. 3A). For example, at an energy state closer to that of resting muscle (ΔG_{ATP}=–14.0 kcal mol^{-1}), pyruvate utilization decreases 67±4% when both palmitoyl-L-carnitine and glutamate are also available. But at an energy state associated with moderate intensity locomotion (ΔG_{ATP}=–13.0 kcal mol^{-1}), the same additional fuel supply decreased pyruvate utilization 50±3%.

Contributions of pyruvate, glutamate and palmitoyl-L-carnitine to substrate oxidation

The average relative contribution of each fuel to oxygen consumption is presented in Figs. 4 and 5. In sparrow mitochondria, fatty acid consistently provided the majority of the fuel regardless of energy state, while pyruvate contributed very little (Fig. 5B–D). Glutamate competed slightly more successfully with fatty acids than pyruvate, but nevertheless failed to make more than a minor contribution under any energetic condition (Fig. 5B–D). In dramatic contrast, rat mitochondrial fuel metabolism was dominated by pyruvate and glutamate (Fig. 5A–D). While, as noted above, fatty acid out-competed pyruvate under high ATP energy (low flux) conditions, it is much less successful against glutamate, especially as ATP free energy was relaxed and flux rose (Fig. 5C). The delivery of 'glycolytic pathway products' (the combination of pyruvate and glutamate) to rat muscle mitochondria nearly abolished fatty acid metabolism under all energetic conditions (Fig. 5D).

Table 3. Ratio of mean steady-state J_O at a given value of ΔG_{ATP} to the V_{max} J_O determined from Eadie–Hofstee analysis

	J_O/V_{max} J_O (%)	
ΔG_{ATP} (kcal mol^{-1})	Rat	Sparrow
–13.0	86±2	69±4
–13.5	75±4	53±4
–14.0	60±6	36±5

Values represent the mean (± s.e.m.) of all fuel combinations at a given ΔG_{ATP}. Data for individual fuel combinations can be found in supplementary material Table S2.

ETC conductance

A linear thermodynamic force:metabolic flow (ΔE_h:J_O) relationship was observed for NADH oxidation in sonicated mitochondria from both rat and sparrow (Fig. 6A). A slight loss of linearity, suggesting kinetic saturation, was seen at the highest ΔE_h and J_O values. Eliminating these data improved the fit of the regression and did not affect the differences between the species. The slope of the ΔE_h:J_O relationship was 1.7-fold higher in sparrow than in rat mitochondria (14,589±1811 versus 8797±1322, respectively); these slopes converted to proportional conductance units gave values of 94±12 versus 57±9 mS mg^{-1}, respectively (Fig. 6A,C). Additionally, the V_{max} of NADH oxidation was over 2 times greater in sparrow mitochondria (1074±118 versus 516±42 nmol O_2 min^{-1} mg^{-1}, respectively) (Fig. 6B).

DISCUSSION

Three fundamental functional differences between avian and mammalian skeletal muscle mitochondria were revealed by these studies. (1) Mammalian mitochondria control respiration over a more negative range of ATP free energy. In more familiar kinetic terms, the $K_{m,ADP}$ for respiration is lower in rat than in sparrow muscle mitochondria. This is particularly the case when fatty acid was the respiratory substrate. (2) Avian mitochondria primarily oxidize fatty acids and strongly spare pyruvate from oxidation across all energy states. The ability of a fuel to outcompete another for oxidation was not the simple consequence of a higher V_{max}. (3) Avian mitochondria possess much greater conductance for electron flow down the ETC, suggesting that a given $\dot{V}_{O_2}$ can be achieved with a more oxidized matrix, i.e. higher NAD^+/NADH ratio [at any given level of downstream backpressure exerted by the protonmotive force (Δp) and ATP free energy].

Substrate additivity versus competition

Previous *in vitro* studies of mitochondrial fuel selection (Ashour and Hansford, 1983) established a constant ATP turnover rate by subjecting mitochondria to an ATP-splitting enzyme system (e.g. hexokinase + glucose). The mitochondrial response to elevated ATP demand therefore included not only fuel selection but also concentration control of the ATP/ADP ratio. Our objective was to instead assess the effect of fuel availability on fuel oxidation rates at experimentally clamped energy states (ATP/ADP ratios). In this

The Journal of Experimental Biology (2014) doi:10.1242/jeb.098863

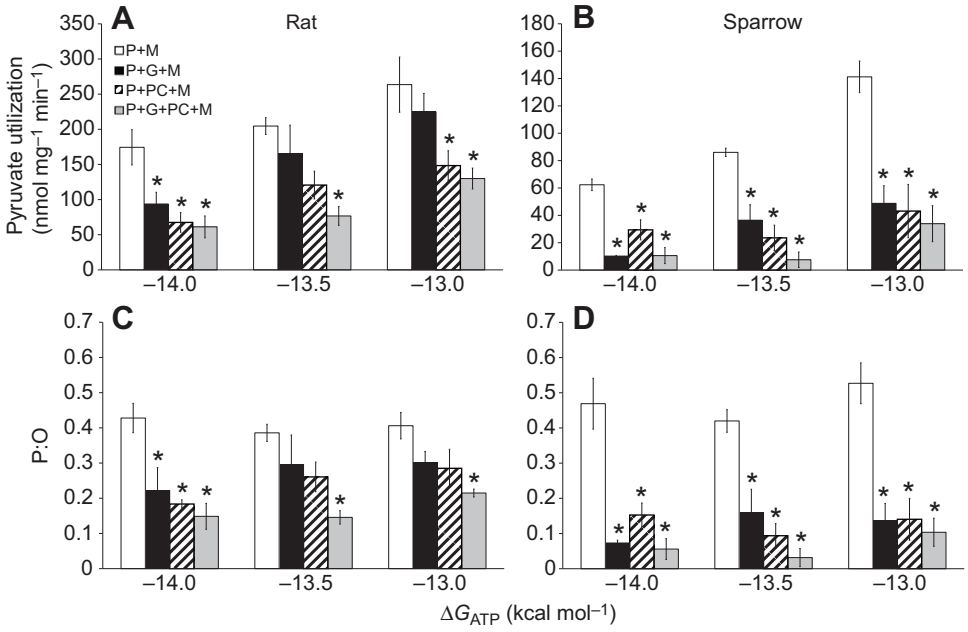

Fig. 2. Pyruvate utilization rates. Absolute rate of pyruvate utilization for rat (A) and sparrow (B) and pyruvate utilization rate normalized to oxygen consumption rate (P:O) for rat (C) and sparrow (D) during steady-state respiration at three values of ΔG_{ATP}. Fuel combinations are P+M, P+G+M, P+PC+M and P+G+PC+M. Values represent means ± s.e.m. *Significantly different from P+M at the same ΔG_{ATP}. *N*=4 rats, *N*=3 sparrows.

approach, because the energy clamp has complete concentration control, the mitochondria have complete control of flux (Cornish-Bowden, 1999; Messer et al., 2004). The clamp controlled the free energy of ATP at one of three levels, −14.0, −13.5 or −13.0 kcal mol^{-1}; a less negative value means less 'backpressure' from downstream ATP opposing oxidative flux (Davis and Davis-van Thienen, 1989). According to the chemiosmotic theory (see Fig. 7B), flux reflects the disequilibrium between this fixed downstream backpressure versus the upstream 'input pressure' developed by the oxidation of added substrate(s) (Koretsky and Balaban, 1987; Messer et al., 2004). Fuel B added to an incubation in which mitochondria are oxidizing fuel A will thus either simply add J_O flux, or B will compete with A, depending on the interplay between the fuels and their interactions with the citric acid cycle. Measurements of the rates of O_2 consumption and fuel utilization thus provide a clear evaluation of the extent to which substrates either add together (additivity) or compete with one another to develop the matrix redox pressure. Two cases provide illustrative examples. (1) In rat muscle mitochondria, fatty acid (PC) added to pyruvate + malate (P+M) does not add flux (Fig. 1C, Table 2). This suggests that PC simply competes with pyruvate to develop the matrix redox developed by P+M (Fig. 7A). These two pathways merge at acetyl-CoA, which has long been considered an important locus of control in the selection of carbohydrate versus fat (see below). (2) Flux rises when glutamate is added to P+M (Fig. 1C, Table 2). This additivity is observed at all energy states in both species, but additivity is particularly prominent in sparrow (Fig. 1C,D). Indeed, the addition of glutamate to P+M increased the calculated V_{max} 96% in sparrow mitochondria, but only 13% in rat mitochondria (Table 2). The oxidative pathways of glutamate and pyruvate might compete because they share a dependence on oxaloacetate (OAA) availability; pyruvate oxidation requires the citrate synthase reaction and glutamate oxidation in muscle requires the aspartate aminotransferase reaction (Fig. 7A). In turn, the matrix [OAA] depends on two distinctive features of the malate dehydrogenase (MDH) reaction: a very large positive standard free energy in the direction of OAA formation and an extremely high MDH V_{max}, which maintains near-equilibrium in the reaction (Williamson, 1979). As a result, matrix [OAA] is maintained at very low micromolar levels and varies according to the matrix redox state:

$$[\mathrm{OAA}] = K_{eq} \times [\mathrm{M}] \times \mathrm{NAD}^+ / \mathrm{NADH}\,, \quad (1)$$

in which the K_{eq} is in the vicinity of 10^{-5}. Thus, if small decreases in matrix NAD^+/NADH elicit large increases in electron flux toward complex IV, in other words if the ETC has high electron conductance, then glutamate addition to P+M would more likely increase flux, rather than compete with pyruvate by diminishing matrix [OAA]. The observation made here that avian mitochondria exhibit marked additivity of flux when glutamate is added to P+M is therefore consistent with the observed much higher avian ETC conductance for electron transport. Indeed, additivity of multiple

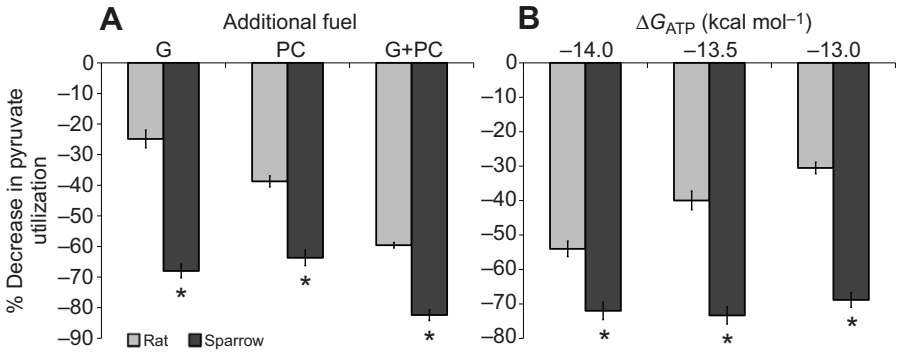

Fig. 3. Change in pyruvate utilization with additional fuel. (A) Average decrease in pyruvate utilization at all energy states by the addition of G, PC or G+PC to P+M oxidation. (B) Average decrease in pyruvate utilization with any additional fuel across ΔG_{ATP}. Values represent means ± s.e.m. *Significantly greater decrease in pyruvate utilization versus rat. *N*=4 rats, *N*=3 sparrows.

The Journal of Experimental Biology (2014) doi:10.1242/jeb.098863

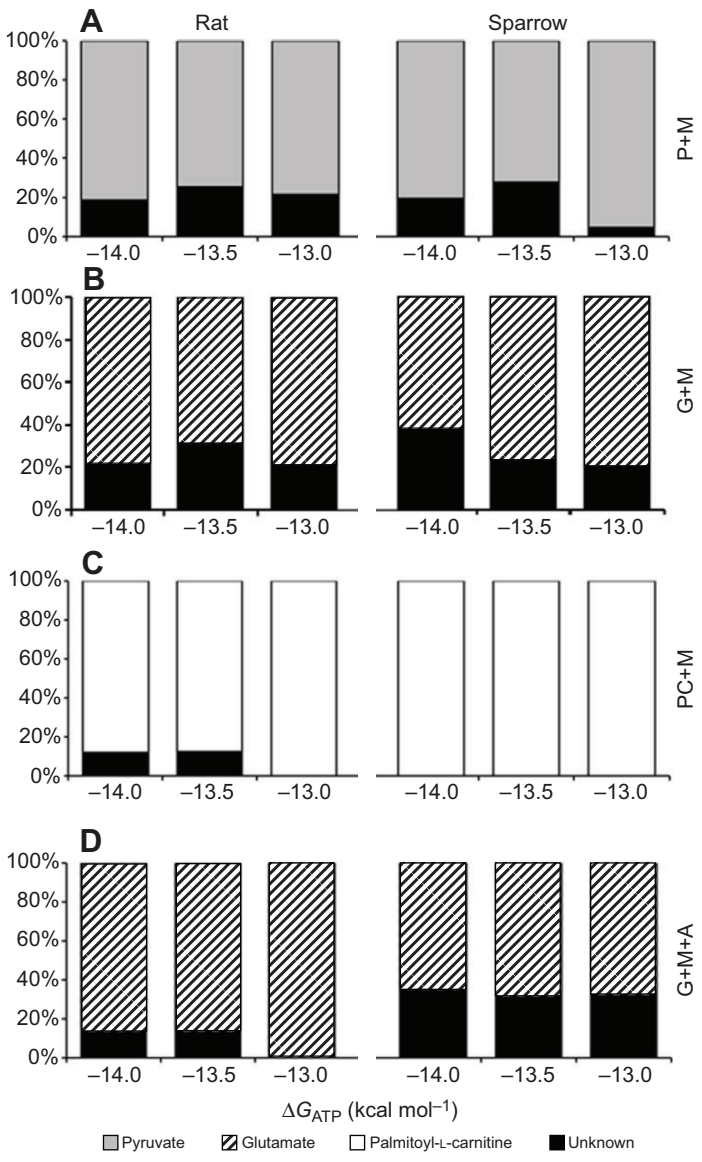

Fig. 4. Fuel contribution to J_O. Relative contributions of fuels to oxygen consumption rate at three values of ΔG_{ATP} in rat and sparrow. Fuel combinations: (A) P+M, (B) G+M, (C) PC+M and (D) G+M+A. Fuel contributors to J_O are P, G, PC and unknown. Fuel contribution calculations are as described in Materials and methods. *N*=4 rats, *N*=3 sparrows.

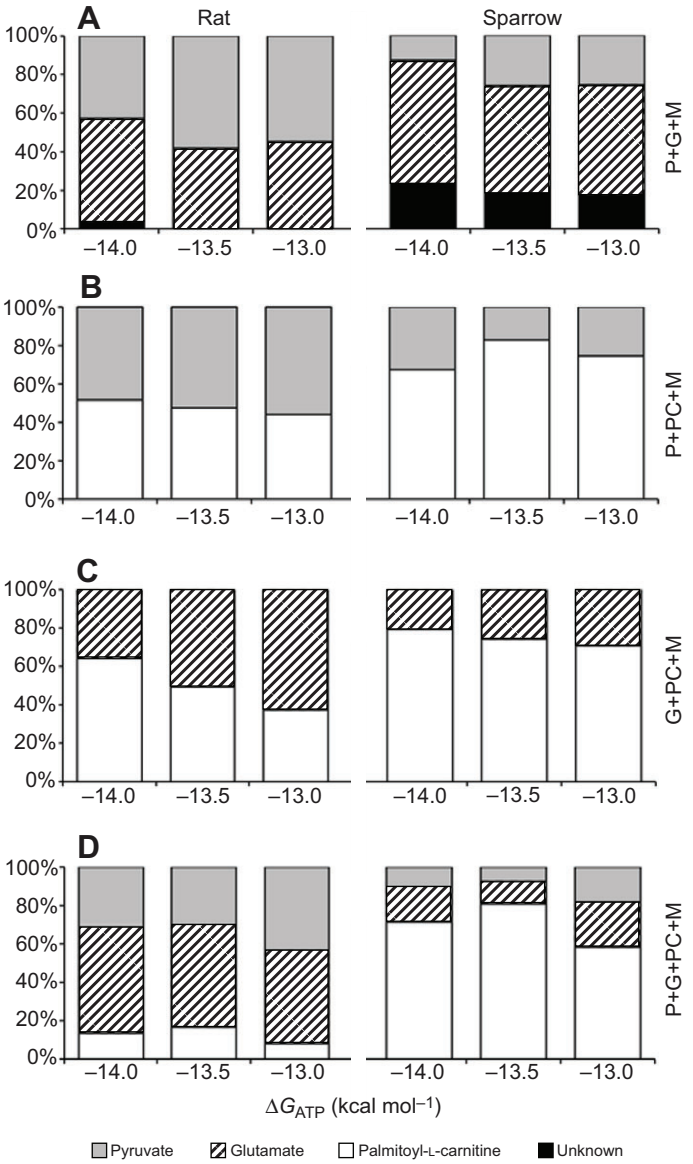

Fig. 5. Fuel contribution to J_O. Relative contributions of fuels to oxygen consumption rate at three values of ΔG_{ATP} in rat and sparrow. Fuel combinations: (A) P+G+M, (B) P+PC+M, (C) G+PC+M and (D) P+G+PC+M. Fuel contributors to J_O are P, G, PC and unknown. Fuel contribution calculations are as described in Materials and methods. *N*=4 rats, *N*=3 sparrows.

substrates was generally evident in sparrow mitochondrial incubations (Table 2).

Control of respiration

For almost all fuels and combinations, the $K_{m,ADP}$ was higher in sparrow than in rat mitochondria (Table 2), indicating the sparrow controls respiration over a greater range of ΔG_{ATP}. At the three values of ΔG_{ATP} investigated in the present study, sparrow mitochondria were operating at a lower percentage of V_{max} (Table 3). It is therefore likely that ΔG_{ATP} can fall lower in sparrow than in rat mitochondria and still maintain useful contractile function. It is also likely that sparrow mitochondria energy production is activated by both [ADP] and [P_i]. The experiments in the present study employ a [P_i] of 10 mmol l^{-1}. In unpublished experiments from our lab (S.K.-G. and D. L. Gardner), we found that NAD-linked isocitrate dehydrogenase (IDH), which is activated by ADP in mammalian mitochondria, is dependent on [P_i] in sparrow mitochondria over the range 0–25 mmol l^{-1}. In fact, in the absence of P_i, IDH activity was undetectable, corroborating very low rates reported for whole muscle (Alp et al., 1976). This suggests an activation of NADH production by rising [P_i] before ΔG_{ATP} falls significantly.

It is also important to point out that compared with mammalian limb muscle that supports locomotion, avian pectoralis muscle has a much higher mass-specific ATP turnover rate. The maximal (state 3) mitochondrial oxygen consumption rate expressed per mg of mitochondrial protein is not very different between these species (Table 2; supplementary material Fig. S1) (Kuzmiak et al., 2012). As such, the energy requirements of flight can only be met because of the higher mitochondrial volume and protein density of avian myocytes. As pioneered by Weibel and colleagues and examined for

The Journal of Experimental Biology (2014) doi:10.1242/jeb.098863

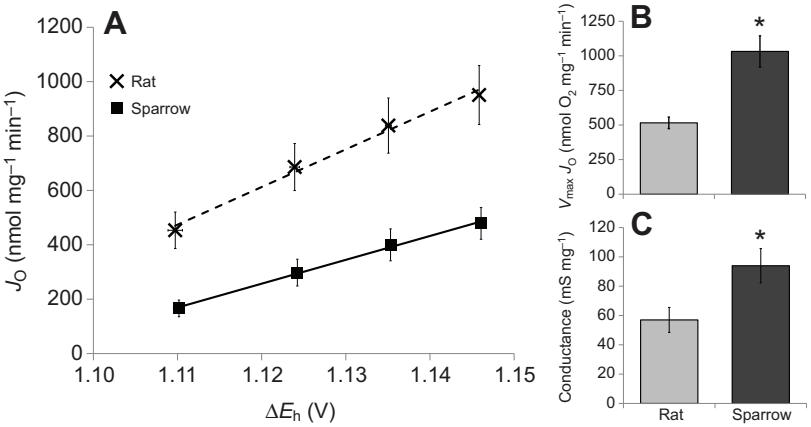

Fig. 6. Electron transport chain (ETC) conductance. (A) Linear relationship between J_O and redox potential difference (ΔE_h) down the ETC was observed in both rat and sparrow mitochondria. The slopes were significantly different: 14,589±1811 for sparrow and 8797±1322 for rat mitochondria. (B) V_{max} J_O fueled by NADH oxidation. (C) Apparent electron conductance from complex I to complex IV in rat and sparrow mitochondria. Values represent means ± s.e.m. *Significantly greater than rat. *N*=6 rats, *N*=8 sparrows.

avian species by our lab, a linear relationship exists between mitochondrial protein density and $\dot{V}_{O2,max}$, demonstrating mammals and birds exhibit similar respiratory capacities per mitochondrial unit (Weibel et al., 1991; Weibel et al., 2004; Kuzmiak et al., 2012).

Avian mitochondria strongly spare pyruvate

The mass-specific rate of energy demand required to support avian flight is enormous (Schmidt-Nielsen, 1984) and the energy density of carbohydrate in its stored, hydrated form is a mere ~1/10 that of lipid (Flatt, 1995; Jenni and Jenni-Eiermann, 1998). Many avian species are able to fly long distances without dietary energy replacement as a result of an almost exclusive reliance on fat oxidation (Rothe et al., 1987). Sparrow mitochondria provided with fatty acid strongly suppressed pyruvate utilization, by 69–78% (Fig. 2B,D), across the entire range of energy states tested. In rat mitochondria, pyruvate sparing was much more flux/energy state dependent: At low ATP turnover (ΔG_{ATP}=–14.0 kcal mol^{-1}), fatty acids inhibited pyruvate oxidation by 60%, consistent with the dominance of fatty acid oxidation in mammalian muscle at rest and during low intensity exercise (Fig. 2A,C) (Romijn et al., 1993; Roberts et al., 1996; Kelley and Mandarino, 2000; Willis et al., 2005). But as energy state was relaxed and the fuel oxidation rate rose, fatty acid addition spared only 30% of the pyruvate oxidized in its absence (Fig. 2A,C). Thus, in the mammalian mitochondria, as the ATP turnover rate increased, pyruvate combustion markedly rose in both absolute and relative terms. Viewed in the other direction, PC accounted for 16% of oxygen consumption at ΔG_{ATP}=–13.0 kcal mol^{-1}, while it accounted for 59% at −14.0 kcal mol^{-1}. These findings are similar to the pyruvate dehydrogenase (PDH) flux results of Ashour and Hansford, who used an ATP-utilizing reaction (hexokinase + glucose) to experimentally establish the *in vitro* rate of ATP turnover (Ashour and Hansford, 1983).

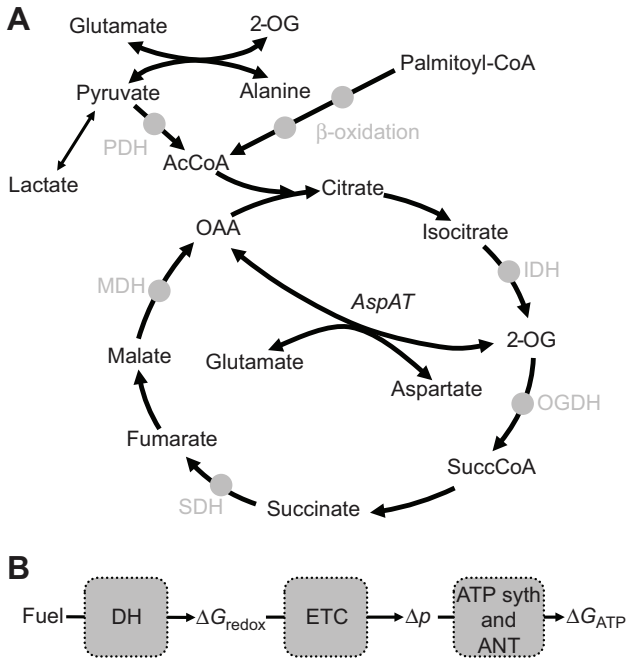

Fig. 7. Schematic representation of the citric acid cycle and chemiosmotic energy transduction. (A) Entry points of carbon and enyzmatic reactions of the citric acid cycle and related enzymes. Fuels were provided as pyruvate, glutamate or palmitoyl-L-carnitine, which is converted to palmitoyl-CoA by carnitine palmitoyl transferase II before undergoing β-oxidation. Electron harvesting reactions are indicated by gray circles: pyruvate dehydrogenase (PDH), isocitrate dehydrogenase (IDH), 2-oxoglutarate dehydrogenase (OGDH), succinate dehydrogenase (SDH) and malate dehydrogenase (MDH). (B) Model of the chemiosmotic energy transduction pathway (Mitchell, 1961). The modules represent (1) the substrate dehydrogenase enzymes (DH), (2) the electron transport chain (ETC) and (3) the combined actions of F1-ATP synthase (ATP synth), the phosphate transporter and the adenine nucleotide translocase (ANT). As fuel is broken down, the chemical potential energy is transformed into a redox potential, or ΔG_{redox}. This energy is further transduced into the protonmotive force (Δp) via H^+ pumping as electrons travel down the ETC.

Our results clearly support the contention that fuel competition outcomes are not predictable on the basis of the relative oxidation rates of the individual fuels. For example, in sparrow mitochondria respiring at ΔG_{ATP}=–13.0 kcal mol^{-1}, J_O values with P+M, PC+M and P+PC+M were the same (274, 313 and 315 nmol mg^{-1} min^{-1}, respectively) (Fig. 1D). It is tempting to predict that as all three values were similar, then pyruvate and palmitoyl-L-carnitine made essentially equal contributions when the fuels were combined (along with malate as priming carbon). According to this approach, the fraction contributed by pyruvate is predicted to be 0.47:

$$J_O = \frac{P\,J_O}{(P\,J_O + PC\,J_O)} = \frac{274}{(274+313)} = 0.47\,, \qquad (2)$$

where J_O in this equation represents the O_2 consumed by electrons due to pyruvate oxidation. However, the data show that pyruvate oxidation accounted not for 47% but rather only for 25% of the O_2 consumed under these conditions (Fig. 5B). Apparently, products of fatty acid oxidation inhibit pyruvate oxidation more strongly than they feed back to inhibit their own production. Indeed, it is well known that β-oxidation products, acetyl-CoA and NADH, activate PDH kinase, which phosphorylates and inactivates PDH (Sugden

and Holness, 1994). Acetyl-CoA, and not NADH, seems to be the particularly effective inhibitor; Ashour and Hansford concluded that the active PDH (PDH_A) decrease attending palmitoyl-L-carnitine addition tracked the acetyl-CoA/CoA ratio and not the $NADH/NAD^+$ ratio (Ashour and Hansford, 1983).

Suppression of fat oxidation by matrix redox

In mammals, fat oxidation rate rises with exercise intensity, as long as the intensity remains within the mild to moderate range (Romijn et al., 1993; Willis et al., 2005), i.e. at intensities below the lactate threshold. Across this range, myocyte $NAD^+/NADH$ also rises (Sahlin et al., 1987). At intensities exceeding roughly 60–70% $\dot{V}_{O2,max}$, i.e. the lactate threshold, however, myocyte $NAD^+/NADH$ falls (Sahlin et al., 1987), as does the fat oxidation rate (Jones et al., 1980; Romijn et al., 1993). There is evidence that mitochondrial fatty acid oxidation is actively suppressed at these high intensities (Romijn et al., 1995), but the mechanism proposed, that of malonyl-CoA inhibition at carnitine palmitoyl transferase I (CPT-I), is not consistent with the observation that malonyl-CoA levels fail to change in the predicted direction (Winder et al., 1989; Odland et al., 1996).

An alternative mechanism is, however, supported by available evidence in a compelling fashion. The falling myocyte $NAD^+/NADH$ levels, associated with over tenfold increases in muscle lactate:pyruvate ratios (Sahlin et al., 1987), reflect a fundamental requirement for aerobic glycolysis: the shuttling of cytosolic NADH electrons into mitochondria. Almost 40 years ago, Lumeng et al. demonstrated in rat liver mitochondria incubated with saturating levels of palmitoyl-L-carnitine that the reconstruction of the malate–aspartate electron shuttle abolished fatty acid oxidation (Lumeng et al., 1976). Fat oxidation was also completely inhibited when the glycerol 3-phosphate (G3P) electron shuttle was fueled in liver mitochondria isolated from rats pre-treated with thyroid hormone, which upregulates hepatic mitochondrial G3P dehydrogenase. In both cases, β-oxidation pathway flux decreased as the matrix NADH/NAD ratio increased. Sahlin's laboratory has also suggested the possibility of control of β-oxidation flux by $NADH/NAD^+$ (Mogensen and Sahlin, 2005). In the present study, as in the study by Lumeng et al. (Lumeng et al., 1976), fatty acid was provided to mitochondria as PC, which bypasses CPT-I entirely. Corroborating Lumeng et al., glutamate addition to fuel the mitochondrial steps of the malate–aspartate shuttle (Bookelman et al., 1979) suppressed fatty acid utilization concomitant with markedly increased J_O flux, which is consistent with an elevated matrix redox pressure. This pattern was dramatically the case in mammalian mitochondria, while it occurred to a minor extent in avian mitochondria. The findings above strongly suggest that fatty acid oxidation may be a more competitive substrate in sparrow mitochondria because of their very high ETC electron conductance.

In both species, electron flow down the ETC is a linear function of the driving force (ΔE_h) (Fig. 6), providing a compelling example of a pathway flux conforming to a linear thermodynamic force:metabolic flow relationship (Rottenberg, 1973; Van der Meer et al., 1980; Kushmerick et al., 1992; Glancy et al., 2013). V_{max} J_O in disrupted mitochondria oxidizing NADH was higher in sparrow than in rat, in agreement with previous avian mammalian comparisons (Rasmussen et al., 2004; Kuzmiak et al., 2012). This greater catalytic potential in avian ETC might facilitate at least two functional outcomes. First, during routine flight, sparrow pectoralis mitochondria could generate a high ETC flux at a low matrix redox potential, which would minimize inhibition of β-oxidation, allowing fatty acids to produce acetyl-CoA and inhibit pyruvate oxidation. Second, under conditions of rising lactate availability due, for example, to a rapid glycogenolysis proceeding in the same or another cell (Rothe et al., 1987), glycolytic products (pyruvate and the malate–aspartate shuttle) would additively fuel a yet higher rate of oxidative phosphorylation. Our data show that bird mitochondria oxidizing a single substrate increase V_{max} J_O by 50% when multiple substrates are added, in comparison with an 11% increase in rat mitochondria (Table 2).

Summary

Mitochondrial fuel oxidation and selection mirrored that of the whole body: in rat mitochondria the reliance on carbohydrate increased and the relative contribution of fat decreased as the rate of oxygen consumption increased, whereas fat dominated under all conditions in the sparrow. This indicates that fuel selection, at least in part, can be modulated at the level of the mitochondrial matrix when multiple substrates are present at saturating levels. As an increase in matrix redox potential has been linked to a suppression of palmitoyl-L-carnitine (Lumeng et al., 1976), we suggest a high ETC conductance relative to dehydrogenase activity in avian compared with rat mitochondria observed by our lab and others (Rothe et al., 1987) may result in a selective oxidation of fatty acids for energy in avian compared with mammalian mitochondria.

MATERIALS AND METHODS

Animals

All procedures are in accordance with the guiding principles in the care and use of animals at Arizona State University. House sparrows (*P. domesticus*) were captured at a Livestock Auction (Phoenix East Valley, AZ, USA) by mist net the morning of each experiment. The sparrows, weighing 21–28 g, were fasted for 2–3 h during transport to the laboratory. Sprague–Dawley rats (*R. norvegicus*, weighing 300–400 g) and sparrows were killed with an overdose of CO_2. Pectoralis muscle was extracted and removed from the keel of a sparrow and the quadriceps femoris and triceps surae groups were extracted from the rats. These species were chosen as (1) a characterization of the oxygen consumption and reactive oxygen species production in these species was previously conducted (Kuzmiak et al., 2012), (2) rat hindlimb muscle provided adequate tissue for mitochondrial isolation and functional assessment, (3) the fuel mixture oxidized by the rat is representative of mammalian patterns, (4) the glucose and fatty acid uptake by sparrow muscle has been previously examined (Sweazea and Braun, 2005; Sweazea and Braun, 2006) and (5) there is no apparent correlation between body mass and mitochondrial oxygen consumption rate (Rasmussen et al., 2004). Extracted muscles were immediately placed in an ice-cold solution of (in mmol l^{-1}) 100 KCl, 40 TrisHCl, 10 Tris base, 5 $MgCl_2$, 1 EDTA and 1 ATP, pH 7.4 (solution I) (Makinen and Lee, 1968) and mitochondria were isolated as described previously (Kuzmiak et al., 2012). Protein concentrations of the final mitochondrial suspensions were 15.0±1.3 and 8.4±0.9 mg mitochondrial protein ml^{-1} for sparrows and rats, respectively.

Mitochondrial oxygen consumption and fuel utilization

Respiration studies were performed in ~2.0 ml of a respiration medium (RM) containing (in mmol l^{-1}) 100 KCl, 50 MOPS, 20 glucose, 10 KPO_4, 10 $MgCl_2$ and 1 EDTA, with 0.2% BSA, pH 7.0. A Clark-type O_2 electrode was used to measure mitochondrial O_2 consumption (J_O) at 37°C (Rank Brothers, Cambridge, UK) as described previously (Messer et al., 2004). Other assay conditions and substrate additions are as noted in the legends of figures and tables.

Creatine kinase energy clamp

Steady-state respiratory rates (J_O) intermediate to the maximum rate (state 3) and resting rate (state 4) were established by incubating mitochondria over a range of energetic states using a modification of the creatine kinase (CK) energetic clamp described previously (Messer et al., 2004). Incubations were primed with 5 mmol l^{-1} creatine (Cr), 5 mmol l^{-1} ATP, 10 mmol l^{-1} P_i

and excess CK. Separate incubations contained 2.5, 5 or 10 mmol l^{-1} phosphocreatine (PCr) to obtain PCr/Cr ratios of 0.5, 1.0 or 2.0. Because incubations were buffered at pH 7.0, the equilibrium constant of the CK reaction (K_{ck}):

$$K_{ck} = \frac{[Cr][ATP]}{[PCr][ADP][H^+]}, \quad (3)$$

in which K_{ck} equals 1.77×10^9 (Teague et al., 1996), and reduces to a value of 177 with $[H^+]$ maintained at 10^{-7} mol l^{-1}. Thus, the ATP/ADP ratio was experimentally established (clamped) with appropriate additions of PCr and Cr as:

$$\frac{[ATP]}{[ADP]} = 177\frac{[PCr]}{[Cr]}. \quad (4)$$

At an experimentally clamped ATP/ADP ratio, the Gibbs free energy of ATP (ΔG_{ATP}) is calculated as:

$$\Delta G_{ATP} = RT\ln\frac{\Gamma}{K_{ATP}}, \quad (5)$$

in which the mass action ratio, Γ, of the ATP hydrolysis reaction is:

$$\Gamma = \frac{[ADP][P_i]}{[ATP]}, \quad (6)$$

and K_{ATP}, the equilibrium constant of the ATP hydrolysis reaction, equals 225,000 at pH 7.0 (Teague et al., 1996), R is the gas constant (1.987 cal K^{-1} mol^{-1}) and T is the temperature in Kelvin (310 K). Thus, PCr/Cr ratios of 0.5, 1.0 and 2.0 resulted in ATP/ADP ratios of 75, 150 and 300, respectively, with corresponding final [ADP] of 66.7, 33.3 and 16.7 μmol l^{-1}. At the incubation $[P_i]$ of 10 mmol l^{-1}, these energy phosphate conditions resulted in ΔG_{ATP} values of −13.0, −13.5 and −14.0 kcal mol^{-1}, respectively.

Oxidative substrates

Substrates provided to respiring mitochondria, either alone or in combination, included 0.5 mmol l^{-1} P, 5.0 mmol l^{-1} G and 10 μmol l^{-1} PC. Importantly, PC is translocated directly into the mitochondrial matrix in exchange for carnitine, i.e. fat metabolism in these studies did not involve CPT-I. In all incubations, the citrate cycle was primed with 0.5 mmol l^{-1} M. After malate priming, fuels were provided alone as P+M, G+M or PC+M, as well as in combination as P+G+M, P+PC+M, G+PC+M or P+G+PC+M. Additionally, G+M was added with 2.0 mmol l^{-1} A, which specifically reconstructs the mitochondrial steps of the malate–aspartate shuttle. Arsenite inhibition of OGDH ensures that the MDH reaction Mal + NAD^+ → OAA + NADH is the sole site generating reducing power, as glutamate transaminates with OAA to form 2-OG and aspartate and the formed 2-OG and aspartate then exchange with extra-mitochondrial malate and glutamate, respectively. The G3P shuttle was not assessed as previous work indicates it does not operate in sparrow mitochondria (Kuzmiak et al., 2012).

Substrate competition assays

Timed incubations were carried out to determine fuel oxidation rates. The energy clamp components and substrates were added to the incubation medium and, after a few minutes equilibration period, the incubation was initiated by the addition of ~200 μg mitochondrial protein. A 'pre-incubation' sample (500 μl) was immediately withdrawn and quenched in 150 μl 25% $HClO_4$ and J_O was followed continuously until a second 'post-incubation' aliquot was similarly sampled and quenched. Incubations were ~10 min in duration; all durations were precisely measured and recorded times were used to calculate substrate fluxes. Acidified samples were promptly centrifuged for 1.0 min at 14,000 ***g*** and supernatants were neutralized with 2 mol l^{-1} KOH + 0.5 mol l^{-1} MOPS. An aliquot of this acid/neutralized extract was stored on ice to fluorometrically assay for pyruvate on the same day; the remainder was stored at −80°C for subsequent metabolite analyses.

For each fuel combination, J_O was plotted against ΔG_{ATP} to obtain the thermodynamic force:metabolic flow relationship, a measure of mitochondrial sensitivity to a respiratory signal. Using the same data set, $K_{m,ADP}$ and V_{max} J_O were determined using Eadie–Hofstee analysis, plotting J_O against J_O/[ADP].

Metabolite assays

All metabolite assays were carried out by enzymatically linking substrate metabolism to the oxidation/reduction of NAD^+/NADH by fluorescence changes (excitation λ 360 nm, emission λ 465 nm) in a 96-well microplate reader (TECAN GENios, Durham, NC, USA). Assays were run in duplicate using 10–40 μl of acidified/neutralized extract in a final assay volume of 200 μl. Standard curves were run daily. Pyruvate was assayed by a method adapted from a previous publication (Bergmeyer and Bernt, 1974). Malate, 2-OG and aspartate assays were adapted from Williamson and Corkey (Williamson and Corkey, 1969). Preliminary experimental incubations were assayed for OAA, citrate, isocitrate, lactate and alanine, and these metabolites did not show measurable accumulation with any substrate or substrate combination used (data not shown). Net metabolite disappearance and appearance rates were expressed per mg of mitochondrial protein in the incubation and can be found in supplementary material Table S3.

Fuel utilization calculations

The net contributions of pyruvate, glutamate and palmitoyl-L-carnitine to the mitochondrial fuel supply were based on the principle of mass balance and the measured rates of O_2 consumption, pyruvate utilization, malate utilization and aspartate formation (see Fig. 7A). For these calculations, O_2 consumption rates and substrate utilization and formation rates were averaged for each condition so the data represent the mean for all experiments. In these fuel-utilization studies, 100–200 μg of mitochondrial protein was incubated in a 2 ml incubation system sealed from the environment. This quantity of mitochondria carries with it essentially no stored oxidizable substrates (Messer et al., 2004). All reducing equivalents available to the mitochondria were therefore experimentally controlled as fuel added in the form of malate, pyruvate, glutamate and/or palmitoyl-L-carnitine. In this highly controlled environment, the total O_2 consumed provides the total number of electron pairs extracted from added fuels. As seen in Fig. 7A, the pyruvate and palmitoyl-L-carnitine pathways converge at acetyl-CoA; thus, both require OAA to advance to citrate via the citrate synthase reaction. In turn, OAA is derived from malate, which was added to prime the citrate cycle at 0.50 mmol l^{-1}. Glutamate metabolism also utilizes malate priming carbon when it transaminates with OAA to form aspartate and 2-OG. Thus, the metabolism of all three substrates involves 2-OG formation, which can either be oxidized at OGDH or exchanged with extra-mitochondrial malate via the dicarboxylate carrier into a vast volume of respiration medium where it would accumulate. Net 2-OG accumulation was measured to assess the extent to which carbon either exited the mitochondrial matrix or advanced through OGDH into the second span of the citrate cycle. Please contact corresponding author for details on fuel utilization calculations. Briefly, the approach and assumptions on which these calculations are based can be fairly described as a process that rigorously assesses the contributions of pyruvate and glutamate oxidation to fuel metabolism, and thus uses O_2 consumption and mass balance to estimate the reducing equivalents generated by the β-oxidation of fatty acids.

NADH oxidation in disrupted mitochondria

NADH oxidation by sonicated mitochondria assessed the electron conductance of the ETC from complex I to complex IV. Frozen mitochondria were diluted 50% with 10 mmol l^{-1} KPO_4, pH 7.0, and sonicated in three, 10 s bouts with a Branson Sonifier at 40% power; the mitochondria were rested on ice for 5 min between each bout. The assay began with 2.0 ml RM to which was added ~100 μg of sonicated mitochondrial protein followed by a 750 nmol bolus of NADH. The O_2 content of the RM was monitored continuously as it fell exponentially toward a zero slope plateau, indicating the complete oxidation of added NADH. Because of the 1:1 stoichiometry between NADH oxidation to NAD^+ and atomic oxygen reduction to water, the O_2 electrode signal could be used to calculate J_O (hence J_{e-}, the electron current), as well as the ratios of NAD^+/NADH and $½O_2$/H_2O at any point along the progress curve. The total oxygen consumed was determined and the top and bottom 10% of the oxidation curve were excluded. The remaining field was divided into five equally spaced regions and in each both flux (J_O or J_{e-}) and the driving force (the voltage drop) down the ETC were analyzed.

Electron flux, J_O, of a region was determined as the tangential slope at the midpoint O_2 signal of that region. The voltage drop (the redox potential difference, ΔE_h) down the ETC was determined from the NAD^+/NADH and $½O_2/H_2O$ ratios at the midpoint. The redox potential difference (ΔE_h) is:

$$\Delta E_h = E_{h,acceptor} - E_{h,donor} . \quad (7)$$

In turn, the redox potential of the electron acceptor couple at complex IV ($E_{h,acceptor}$), which depends on the $½O_2/H_2O$ ratio, and that of the electron donor at complex I ($E_{h,donor}$), which depends on the NAD^+/NADH ratio, were calculated according to:

$$E_h = E_m + \frac{RT}{nF} \ln \frac{[\text{oxidized}]}{[\text{reduced}]}, \quad (8)$$

where E_m is the midpoint potential (mV), R is the gas constant ($1.987\ \text{cal}\ \text{K}^{-1}\ \text{mol}^{-1}$), T is the temperature in Kelvin (310 K), n is the number of electrons transferred (two in this case) and F is the Faraday constant ($23.062\ \text{cal}\ \text{mV}^{-1}\ \text{mol}^{-1}$). The E_m values used were −320 mV for the NAD^+/NADH couple and +820 mV for the $½O_2/H_2O$ couple. J_O was then plotted against ΔE_h to produce a graph of thermodynamic force: metabolic flow, which was found to be consistently linear (ohmic). After conversion of J_O to J_{e-}, the slope of this ΔE_h:J_{e-} relationship, the apparent conductance of the ETC for electron transfer, was expressed in units of $\text{mS}\ \text{mg}^{-1}$ mitochondrial protein.

Statistics

Differences in the ΔG_{ATP}:J_O slope relationship, V_{max} J_O, $K_{m,ADP}$, and pyruvate utilization within a species were determined using a one-way ANOVA with a Tukey *post hoc* test with $P<0.05$. Independent *t*-tests were used to determine differences in V_{max}, $K_{m,ADP}$, percentage decreases in pyruvate utilization, as well as ETC conductance between the species with $P<0.05$.

Acknowledgements

The authors would like to thank Doree Lynn Gardner for her work on phosphate activation of isocitrate dehydrogenase activity.

Competing interests

The authors declare no competing financial interests.

Author contributions

S.K.-G. performed the experiments, analyzed the data and drafted the manuscript; W.T.W. conceptualized the experiments, guided manuscript development and revised the manuscript.

Funding

This research received no specific grant from any funding agency in the public, commercial or not-for-profit sectors.

Supplementary material

Supplementary material available online at
http://jeb.biologists.org/lookup/suppl/doi:10.1242/jeb.098863/-/DC1

References

Alp, P. R., Newsholme, E. A. and Zammit, V. A. (1976). Activities of citrate synthase and NAD^+-linked and $NADP^+$-linked isocitrate dehydrogenase in muscle from vertebrates and invertebrates. *Biochem. J.* **154**, 689-700.

Andersen, P. and Saltin, B. (1985). Maximal perfusion of skeletal muscle in man. *J. Physiol.* **366**, 233-249.

Ashour, B. and Hansford, R. G. (1983). Effect of fatty acids and ketones on the activity of pyruvate dehydrogenase in skeletal-muscle mitochondria. *Biochem. J.* **214**, 725-736.

Baldwin, K. M., Reitman, J. S., Terjung, R. L., Winder, W. W. and Holloszy, J. O. (1973). Substrate depletion in different types of muscle and in liver during prolonged running. *Am. J. Physiol.* **225**, 1045-1050.

Bergmeyer, H. U. and Bernt, E. (1974). Lactate dehydrogenase. In *Methods of Enzymatic Analysis*, Vol. 2 (ed. H. U. Bergmeyer), pp. 574-579. New York: Academic Press.

Bookelman, H., Trijbels, J. M., Sengers, R. C., Janssen, A. J., Veerkamp, J. H. and Stadhouders, A. M. (1979). Reconstitution of malate-aspartate and alpha-glycerophosphate shuttle activity in rat skeletal muscle mitochondria. *Int. J. Biochem.* **10**, 411-414.

Brooks, G. A. and Donovan, C. M. (1983). Effect of endurance training on glucose kinetics during exercise. *Am. J. Physiol.* **244**, E505-E512.

Brooks, G. A. and Mercier, J. (1994). Balance of carbohydrate and lipid utilization during exercise: the 'crossover' concept. *J. Appl. Physiol.* **76**, 2253-2261.

Butler, P. J., West, N. H. and Jones, D. R. (1977). Respiratory and cardiovascular responses of the pigeon to sustained, level flight in a wind-tunnel. *J. Exp. Biol.* **71**, 7-26.

Chance, B., Leigh, J. S., Jr, Clark, B. J., Maris, J., Kent, J., Nioka, S. and Smith, D. (1985). Control of oxidative metabolism and oxygen delivery in human skeletal muscle: a steady-state analysis of the work/energy cost transfer function. *Proc. Natl. Acad. Sci. USA* **82**, 8384-8388.

Connett, R. J. (1987). Glycolytic regulation during an aerobic rest-to-work transition in dog gracilis muscle. *J. Appl. Physiol.* **63**, 2366-2374.

Cornish-Bowden, A. (1999). Enzyme kinetics from a metabolic perspective. *Biochem. Soc. Trans.* **27**, 281-284.

Dagenais, G. R., Tancredi, R. G. and Zierler, K. L. (1976). Free fatty acid oxidation by forearm muscle at rest, and evidence for an intramuscular lipid pool in the human forearm. *J. Clin. Invest.* **58**, 421-431.

Davis, E. J. and Davis-van Thienen, W. I. (1989). Force-flow and back-pressure relationships in mitochondrial energy transduction: an examination of extended state 3-state 4 transitions. *Arch. Biochem. Biophys.* **275**, 449-458.

Fitts, R. H., Booth, F. W., Winder, W. W. and Holloszy, J. O. (1975). Skeletal muscle respiratory capacity, endurance, and glycogen utilization. *Am. J. Physiol.* **228**, 1029-1033.

Flatt, J. P. (1995). Use and storage of carbohydrate and fat. *Am. J. Clin. Nutr.* **61 Suppl.**, 952S-959S.

Foley, J. M., Harkema, S. J. and Meyer, R. A. (1991). Decreased ATP cost of isometric contractions in ATP-depleted rat fast-twitch muscle. *Am. J. Physiol.* **261**, C872-C881.

Funk, C., Clark, A., Jr and Connett, R. J. (1989). How phosphocreatine buffers cyclic changes in ATP demand in working muscle. *Adv. Exp. Med. Biol.* **248**, 687-692.

Glancy, B., Barstow, T. and Willis, W. T. (2008). Linear relation between time constant of oxygen uptake kinetics, total creatine, and mitochondrial content in vitro. *Am. J. Physiol.* **294**, C79-C87.

Glancy, B., Willis, W. T., Chess, D. J. and Balaban, R. S. (2013). Effect of calcium on the oxidative phosphorylation cascade in skeletal muscle mitochondria. *Biochemistry* **52**, 2793-2809.

Horowitz, J. F., Mora-Rodriguez, R., Byerley, L. O. and Coyle, E. F. (1999). Substrate metabolism when subjects are fed carbohydrate during exercise. *Am. J. Physiol.* **276**, E828-E835.

Hudson, D. M. and Bernstein, M. H. (1983). Gas exchange and energy cost of flight in the white-necked raven, *Corvus cryptoleucus*. *J. Exp. Biol.* **103**, 121-130.

Jeneson, J. A., Westerhoff, H. V., Brown, T. R., Van Echteld, C. J. and Berger, R. (1995). Quasi-linear relationship between Gibbs free energy of ATP hydrolysis and power output in human forearm muscle. *Am. J. Physiol.* **268**, C1474-C1484.

Jenni, L. and Jenni-Eiermann, S. (1998). Fuel supply and metabolic constraints in migrating birds. *J. Avian Biol.* **29**, 521-528.

Jones, N. L., Heigenhauser, G. J., Kuksis, A., Matsos, C. G., Sutton, J. R. and Toews, C. J. (1980). Fat metabolism in heavy exercise. *Clin. Sci. (Lond.)* **59**, 469-478.

Kelley, D. E. and Mandarino, L. J. (2000). Fuel selection in human skeletal muscle in insulin resistance: a reexamination. *Diabetes* **49**, 677-683.

Koretsky, A. P. and Balaban, R. S. (1987). Changes in pyridine nucleotide levels alter oxygen consumption and extra-mitochondrial phosphates in isolated mitochondria: a 31P-NMR and NAD(P)H fluorescence study. *Biochim. Biophys. Acta* **893**, 398-408.

Koutsari, C. and Sidossis, L. S. (2003). Effect of isoenergetic low- and high-carbohydrate diets on substrate kinetics and oxidation in healthy men. *Br. J. Nutr.* **90**, 413-418.

Kushmerick, M. J., Meyer, R. A. and Brown, T. R. (1992). Regulation of oxygen consumption in fast- and slow-twitch muscle. *Am. J. Physiol.* **263**, C598-C606.

Kuzmiak, S., Glancy, B., Sweazea, K. L. and Willis, W. T. (2012). Mitochondrial function in sparrow pectoralis muscle. *J. Exp. Biol.* **215**, 2039-2050.

Lambeth, M. J. and Kushmerick, M. J. (2002). A computational model for glycogenolysis in skeletal muscle. *Ann. Biomed. Eng.* **30**, 808-827.

Lumeng, L., Bremer, J. and Davis, E. J. (1976). Suppression of the mitochondrial oxidation of (-)-palmitylcarnitine by the malate-aspartate and alpha-glycerophosphate shuttles. *J. Biol. Chem.* **251**, 277-284.

Makinen, M. W. and Lee, C. P. (1968). Biochemical studies of skeletal muscle mitochondria. I. Microanalysis of cytochrome content, oxidative and phosphorylative activities of mammalian skeletal muscle mitochondria. *Arch. Biochem. Biophys.* **126**, 75-82.

Mazzeo, R. S., Brooks, G. A., Schoeller, D. A. and Budinger, T. F. (1986). Disposal of blood [1-13C]lactate in humans during rest and exercise. *J. Appl. Physiol.* **60**, 232-241.

Messer, J. I., Jackman, M. R. and Willis, W. T. (2004). Pyruvate and citric acid cycle carbon requirements in isolated skeletal muscle mitochondria. *Am. J. Physiol.* **286**, C565-C572.

Mitchell, P. (1961). Coupling of phosphorylation to electron and hydrogen transfer by a chemi-osmotic type of mechanism. *Nature* **191**, 144-148.

Mogensen, M. and Sahlin, K. (2005). Mitochondrial efficiency in rat skeletal muscle: influence of respiration rate, substrate and muscle type. *Acta Physiol. Scand.* **185**, 229-236.

O'Brien, M. J., Viguie, C. A., Mazzeo, R. S. and Brooks, G. A. (1993). Carbohydrate dependence during marathon running. *Med. Sci. Sports Exerc.* **25**, 1009-1017.

Odland, L. M., Heigenhauser, G. J., Lopaschuk, G. D. and Spriet, L. L. (1996). Human skeletal muscle malonyl-CoA at rest and during prolonged submaximal exercise. *Am. J. Physiol.* **270**, E541-E544.

Rasmussen, U. F., Vielwerth, S. E. and Rasmussen, H. N. (2004). Skeletal muscle bioenergetics: a comparative study of mitochondria isolated from pigeon pectoralis,

rat soleus, rat biceps brachii, pig biceps femoris and human quadriceps. *Comp. Biochem. Physiol.* **137A**, 435-446.
Richardson, R. S., Poole, D. C., Knight, D. R., Kurdak, S. S., Hogan, M. C., Grassi, B., Johnson, E. C., Kendrick, K. F., Erickson, B. K. and Wagner, P. D. (1993). High muscle blood flow in man: is maximal O2 extraction compromised? *J. Appl. Physiol.* **75**, 1911-1916.
Roberts, T. J., Weber, J. M., Hoppeler, H., Weibel, E. R. and Taylor, C. R. (1996). Design of the oxygen and substrate pathways. II. Defining the upper limits of carbohydrate and fat oxidation. *J. Exp. Biol.* **199**, 1651-1658.
Romijn, J. A., Coyle, E. F., Sidossis, L. S., Gastaldelli, A., Horowitz, J. F., Endert, E. and Wolfe, R. R. (1993). Regulation of endogenous fat and carbohydrate metabolism in relation to exercise intensity and duration. *Am. J. Physiol.* **265**, E380-E391.
Romijn, J. A., Coyle, E. F., Sidossis, L. S., Zhang, X. J. and Wolfe, R. R. (1995). Relationship between fatty acid delivery and fatty acid oxidation during strenuous exercise. *J. Appl. Physiol.* **79**, 1939-1945.
Rothe, H.-J., Biesel, W. and Nachtigall, W. (1987). Pigeon flight in wind tunnel. *J. Comp. Physiol. B* **157**, 99-109.
Rottenberg, H. (1973). The thermodynamic description of enzyme-catalyzed reactions. The linear relation between the reaction rate and the affinity. *Biophys. J.* **13**, 503-511.
Sahlin, K., Katz, A. and Henriksson, J. (1987). Redox state and lactate accumulation in human skeletal muscle during dynamic exercise. *Biochem. J.* **245**, 551-556.
Schmidt-Nielsen, K. (1984). *Scaling: Why is Animal Size so Important?* Cambridge: Cambridge University Press.
Sidossis, L. S. and Wolfe, R. R. (1996). Glucose and insulin-induced inhibition of fatty acid oxidation: the glucose-fatty acid cycle reversed. *Am. J. Physiol.* **270**, E733-E738.
Stanley, W. C. and Connett, R. J. (1991). Regulation of muscle carbohydrate metabolism during exercise. *FASEB J.* **5**, 2155-2159.
Stanley, W. C., Gertz, E. W., Wisneski, J. A., Neese, R. A., Morris, D. L. and Brooks, G. A. (1986). Lactate extraction during net lactate release in legs of humans during exercise. *J. Appl. Physiol.* **60**, 1116-1120.
Suarez, R. K., Brown, G. S. and Hochachka, P. W. (1986). Metabolic sources of energy for hummingbird flight. *Am. J. Physiol.* **251**, R537-R542.
Suarez, R. K., Lighton, J. R., Moyes, C. D., Brown, G. S., Gass, C. L. and Hochachka, P. W. (1990). Fuel selection in rufous hummingbirds: ecological implications of metabolic biochemistry. *Proc. Natl. Acad. Sci. USA* **87**, 9207-9210.
Sugden, M. C. and Holness, M. J. (1994). Interactive regulation of the pyruvate dehydrogenase complex and the carnitine palmitoyltransferase system. *FASEB J.* **8**, 54-61.
Sweazea, K. L. and Braun, E. J. (2005). Glucose transport by English sparrow (*Passer domesticus*) skeletal muscle: have we been chirping up the wrong tree? *J. Exp. Zool. A* **303**, 143-153.
Sweazea, K. L. and Braun, E. J. (2006). Oleic acid uptake by in vitro English sparrow skeletal muscle. *J. Exp. Zool. A* **305**, 268-276.
Teague, W. E., Jr, Golding, E. M. and Dobson, G. P. (1996). Adjustment of K′ for the creatine kinase, adenylate kinase and ATP hydrolysis equilibria to varying temperature and ionic strength. *J. Exp. Biol.* **199**, 509-512.
Van der Meer, R., Westeroff, H. V. and Van Dam, K. (1980). Linear relation between rate and thermodynamic force in enzyme-catalyzed reactions. *Biochim. Biophys. Acta* **591**, 488-493.
Wahren, J., Felig, P., Ahlborg, G. and Jorfeldt, L. (1971). Glucose metabolism during leg exercise in man. *J. Clin. Invest.* **50**, 2715-2725.
Walsberg, G. and Wolf, B. (1995). Variation in the respiratory quotient of birds and implications for indirect calorimetry using measurements of carbon dioxide production. *J. Exp. Biol.* **198**, 213-219.
Weibel, E. R., Taylor, C. R. and Hoppeler, H. (1991). The concept of symmorphosis: a testable hypothesis of structure-function relationship. *Proc. Natl. Acad. Sci. USA* **88**, 10357-10361.
Weibel, E. R., Bacigalupe, L. D., Schmitt, B. and Hoppeler, H. (2004). Allometric scaling of maximal metabolic rate in mammals: muscle aerobic capacity as determinant factor. *Respir. Physiol. Neurobiol.* **140**, 115-132.
Williamson, J. R. (1979). Mitochondrial function in the heart. *Annu. Rev. Physiol.* **41**, 485-506.
Williamson, J. R. and Corkey, B. E. (1969). Assays of intermediates of the citric acid cycle and related compounds by fluorometric enzyme methods. In *Methods in Enzymology*, Vol. 13 (ed. J. M. Lowenstein), pp. 434-512. San Diego, CA: Academic Press.
Willis, W. T. and Jackman, M. R. (1994). Mitochondrial function during heavy exercise. *Med. Sci. Sports Exerc.* **26**, 1347-1353.
Willis, W. T., Ganley, K. J. and Herman, R. M. (2005). Fuel oxidation during human walking. *Metabolism* **54**, 793-799.
Winder, W. W., Arogyasami, J., Barton, R. J., Elayan, I. M. and Vehrs, P. R. (1989). Muscle malonyl-CoA decreases during exercise. *J. Appl. Physiol.* **67**, 2230-2233.
Zurlo, F., Larson, K., Bogardus, C. and Ravussin, E. (1990). Skeletal muscle metabolism is a major determinant of resting energy expenditure. *J. Clin. Invest.* **86**, 1423-1427.